**Stanislav KOCMAN, Petr ORSÁG, Jan ŠMÍDA**

VŠB-Technical University of Ostrava

# Analyses of Behaviour of Induction Motor Supplied from Unbalanced Source

***Abstract****. The paper presents results of experimental measurements and computer simulations of an induction motor supplied from a programmable power source enabling an arbitrary adjusting of voltage quality on its output terminals. The tested motor was supplied under chosen levels of voltage unbalance to analyse some of its parameters. Motor simulation model has been also developed using the program EMTP-ATP to compare some its results to results obtained from experimental measurements.*

***Streszczenie.*** *W artykule zaprezentowano wyniki badań eksperymentalnych oraz rezultaty symulacji komputerowej silnika indukcyjnego zasilanego z programowanego źródła mocy umożliwiającego ustawianie dowolnej jakości napięcia. (**Analiza właściwości silnika indukcyjnego zasilanego ze źródła o niezrównoważonych napięciach**)*

**Keywords:** current unbalance, distortion, efficiency, induction motor, voltage unbalance
**Słowa kluczowe:** silnik indukcyjny, nierównowaga napięć

## Introduction

Three-phase squirrel cage induction motors are frequently used for both non-adjustable and adjustable electrical drives. Their large-scale using in various technical applications is given by their simple construction, reliability, low maintenance and relatively low cost. Induction motors implemented into non-adjustable speed drives not using frequency converters for their speed controlling draw current with a low level of distortion primarily depending on quality of the supply voltage, unlike the heavily distorted current drawn by the adjustable speed ones if no filtering technique is used. If the supply voltage is sinusoidal and balanced, the drawn motor current has only very low level of distortion. In this paper, the influence of voltage unbalance on motor current unbalance, motor current distortion, motor speed and motor efficiency is investigated for an induction motor supplied directly from a programmable power source.

Voltage unbalance is one of the voltage characteristics of electrical energy regarded as a power quality problem, which can have serious impacts on electrical devices, e.g. on induction motors. Voltage unbalance causes current unbalance with levels exceeding it several times and giving rise to increased motor heating and current distortion. Unbalance also decreases motor starting and breakdown torques and speed at rated load. As stated in the standard [8], motor permissible power is lower than the rated one in the case when the voltage unbalance is higher than 1%, and induction motor operation is not recommended at voltage unbalance exceeding the value of 5%.

Unbalance in three-phase systems is classified by a coefficient of voltage unbalance. It is defined as negative sequence component divided by positive sequence component:

$$\rho = \left|\frac{\underline{V}_2}{\underline{V}_1}\right| \cdot 100\,(\%) \tag{1}$$

The other definition is from the NEMA standard and from standard [1] using the approximate formula:

$$\rho = \max_i \frac{V_i - V_{\text{avg}}}{V_{\text{avg}}} \cdot 100\,(\%) \tag{2}$$

which is the maximum deviation from the average of three phase voltages divided by this average.

Under normal working conditions, over a week's interval, 95% of all 10-minute average values of unbalance $\rho$ have to be in the range from 0 to 2%, according to the standard EN 50160 [2].

## Tested induction motor

The tested three-phase squirrel cage motor was fed by programmable power source Pacific 3120ASX, a three-phase arbitrary waveform generator with output power up to 12 kVA. Output frequency range is 15-1200 Hz, maximum output phase voltage 270 V and output voltage distortion is below 0.25% (for frequencies 15-200 Hz). The parameters of the tested induction motor are in table 1.

Table 1. The parameters of the motor

| | | | |
|---|---|---|---|
| Rated power | 4 kW | Nominal speed | 1440 rpm |
| Nominal voltage | 400 V | Nominal power factor | 0,81 |
| Nominal current | 8,2 A | Nominal efficiency | 86,6 % |
| Nominal frequency | 50 Hz | Efficiency class | IE 2 |

The measured circuit is shown in Fig. 1.

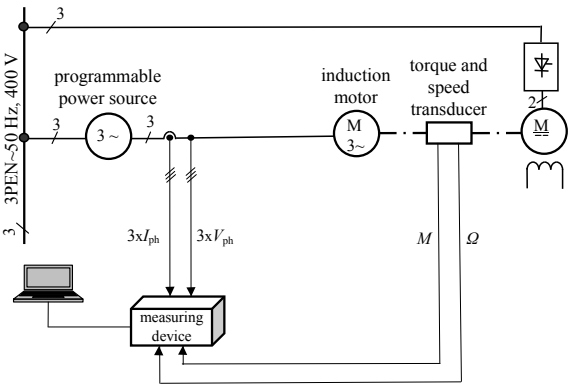


Fig.1. Diagram of the measured circuit

A digital multi-channel measurement system based on two National Instruments DAQ boards NI PCI-MIO16-E1 running parallel, synchronized by RTSI bus was used with a sampling rate of 156,25 kSa/s. Three input voltages were recorded by the first board. Corresponding current signals and both torque and speed signals were recorded by the second board. Three isolation modules DAQP-HV-B were used for signal conditioning of the first board and five isolation modules DAQP-LV-BNC were used for signal conditioning of the second board. All isolation modules, manufactured by Dewetron, are equipped with high

precision signal conditioning amplifiers. The transducer LEM LA 25 NP was used for the measurement of all currents. Torque and speed of the induction motor were measured by HBM T20WN50 transducer. This transducer measures static and dynamic torque and rotation speed or angle of rotation.

**Formulas for calculation of selected characteristic parameters from measured signals**

The input active power of the motor is calculated from the following formula:

$$P_{\text{in}} = \frac{1}{L}\sum_{l=1}^{l=L}\left[v_1(l)\cdot i_1(l) + v_2(l)\cdot i_2(l) + v_3(l)\cdot i_3(l)\right] \tag{3}$$

where: $v$ and $i$ – digitized instantaneous values of phase voltages and currents, $l$ – index of the $l^{\text{th}}$ sample of input voltage and input current, $L$ – number of samples in the interval of observation time.

The mechanical power of the motor is calculated from this formula:

$$P_{\text{m}} = \frac{1}{L}\sum_{l=1}^{l=L}\left[m(l)\cdot\omega(l)\right] \tag{4}$$

where: $m$ – digitized instantaneous value of motor torque, $\omega$ – digitized instantaneous value of motor angular velocity.

Efficiency of the motor is calculated from the following formula:

$$\eta_{\text{m}} = \frac{P_{\text{m}}}{P_{\text{in}}}\cdot 100\ (\%) \tag{5}$$

The input current total harmonic distortion is calculated using the formula:

$$THD_I = \frac{1}{J}\sum_{j=1}^{j=J} THD_{I_j} = \frac{1}{J}\sum_{j=1}^{j=J}\frac{\sqrt{\sum_{h=2}^{h=40} I_{j(\text{h})}^{\,2}}}{I_{j(1)}} \tag{6}$$

where: $j$ – index of the consecutive periods, $J$ – integer number of periods, $h$ – harmonic order, $I_j(h)$ – rms value of the $h^{\text{th}}$ harmonic of current for the $j^{\text{th}}$ period, $I_j(1)$ – fundamental current for the $j^{\text{th}}$ period.

**Experimental measurement results**

Experimental measurements have been performed in our laboratory. The tested induction motor was supplied by almost purely sinusoidal voltage with total harmonic distortion $THD_v$ below 0.2%, at nominal frequency of 50 Hz and under chosen levels of voltage unbalance adjusted on the programmable power source equal to 0%, 1%, 2%, 3%, 4%, 5%, and 10% respectively, which were achieved by voltage decreasing in one phase of the source.

The first detected parameter was motor efficiency which numerous articles deal with, e. g. [3-7]. Its dependence on motor torque under the adjusted levels of voltage unbalance $\rho$ is shown in Fig. 2. As seen in it, voltage unbalance ranging from 0% up to 2% causes almost no reducing of motor efficiency for a specified level of motor loading in its wide range. With higher unbalance levels the efficiency reduction is becoming more evident, approximately in the range from 0.5% to 1%. It can be seen better in Fig. 3 for chosen values of motor load equal to 100%, 75% and 50% of the nominal one. The mechanical characteristic of the tested motor is shown in Fig. 4 for motor torque up to the nominal one presenting its dependence on voltage unbalance as could be expected.

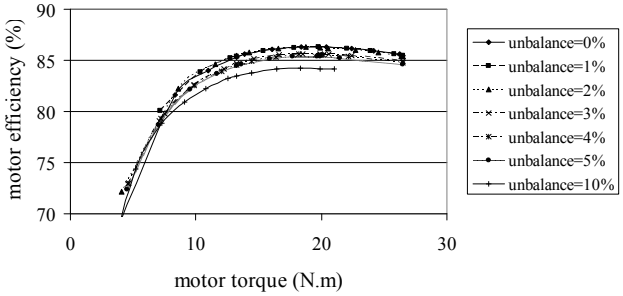


Fig.2. Motor efficiency versus motor torque under adjusted levels of voltage unbalance ($f$=50 Hz, $THD_V$ below 0.2%)

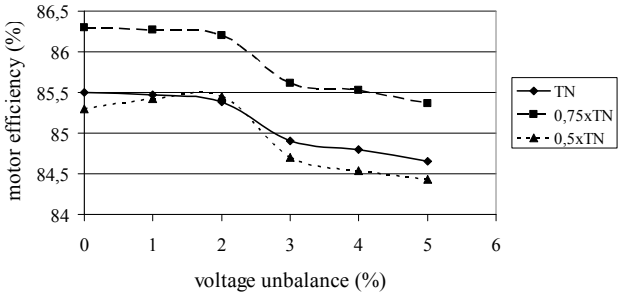


Fig.3. Motor efficiency versus voltage unbalance for chosen values of motor torque ($f$=50 Hz, $THD_V$ below 0.2%)

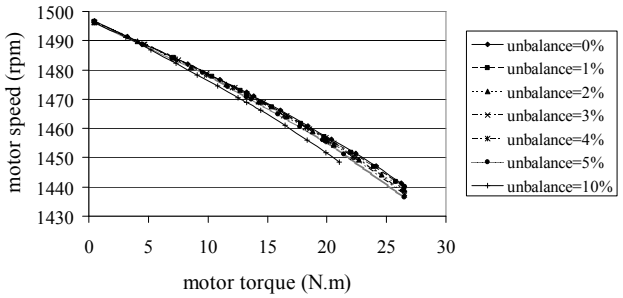


Fig.4. Motor mechanical characteristic under adjusted levels of voltage unbalance ($f$=50 Hz, $THD_V$ below 0.2%)

The voltage unbalance causes extremely high current unbalance exceeding the voltage one c. 6 to 10 times as it is mentioned in the standard [8]. The measured results have not confirmed this mentioned multiple for higher levels of voltage unbalance for all chosen motor loads as seen in Fig. 5. In the case of voltage unbalance being below 2% they match this, but mainly for motor load below the nominal one.

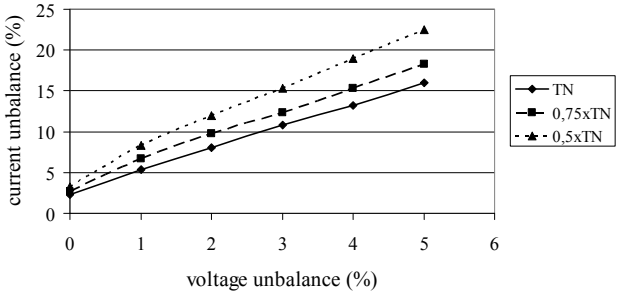


Fig.5. Current unbalance versus voltage unbalance for chosen values of motor torque ($f$=50 Hz, $THD_V$ below 0.2%)

Voltage unbalance range is from 0% to 5%, motor operation at values above 5% is not recommended by the standard [8]. As seen from the Fig.5, voltage balance is not accompanied by the current one, the current unbalance was determined equal to 2.28% for the nominal motor torque.

A current distribution in each phase is in Fig. 6 for voltage unbalance equal to 2%. In this figure a symmetrical current for balanced system is marked for comparison with this distribution.

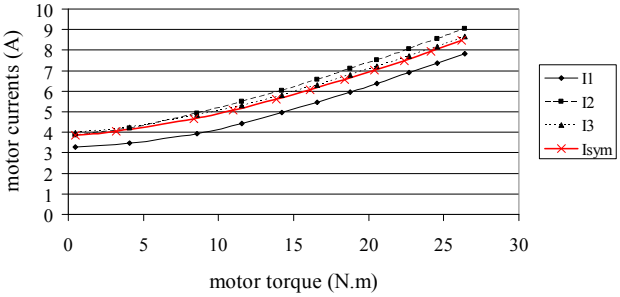


Fig.6. Motor phase currents versus motor torque under voltage unbalance of 2% ($f$=50 Hz, $THD_V$ below 0.2%)

The current in the phase 1 is decreased as the voltage is reduced in it, but causing current increasing in the phase 2 for the same motor torque with exceeding the catalogue value of the nominal current about c.10%. A dependence of the 2nd phase current on motor torque under the adjusted levels of voltage unbalance is shown in Fig. 7 presenting its increasing with unbalance rise leading to increasing of motor heating.

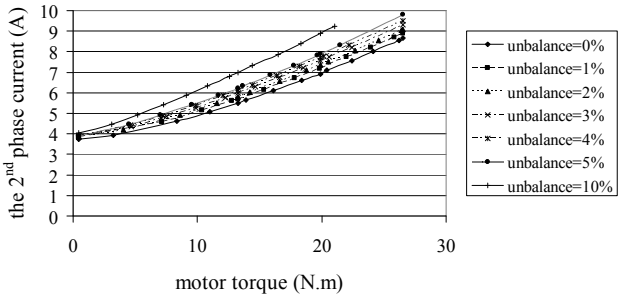


Fig.7. The 2nd phase motor current versus motor torque under adjusted levels of voltage unbalance ($f$=50 Hz, $THD_V$ below 0.2%)

The dependence of the highest drawn current in the 2nd phase on voltage unbalance can be seen in Fig. 8 for chosen values of motor load equal to 100%, 75% and 50% of the nominal one. The overloading of the 2nd phase is evident and is higher in comparison with the phase 3rd, which is more moderate in, as can be seen in Fig. 6 for 2% voltage unbalance.

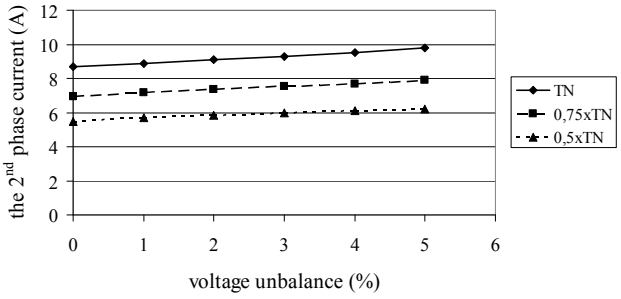


Fig.8. The 2nd phase motor current versus voltage unbalance for chosen values of motor torque ($f$=50 Hz, $THD_V$ below 0.2%)

The tested induction motor was supplied from the programmable power source enabling not only a controlling of output frequency and voltages on adjusted levels, but also supplying the motor by almost purely sinusoidal voltage as mentioned above. Nevertheless, due to certain level of motor asymmetry and its non-linearity the drawn current is not almost purely sinusoidal like voltage, but with a certain level of distortion. However, this distortion level is low with total harmonic distortion $THD_I$ about 2.6% in the case of balanced voltages and nominal load. With unbalance and its rise $THD$ of drawn current also rises up, whereas it is the most progressive in the 3rd phase as can be seen in Fig. 9.

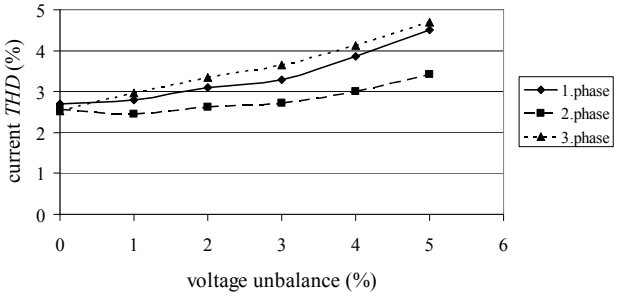


Fig.9. Current $THD$ versus voltage unbalance under nominal torque ($f$=50 Hz, $THD_V$ below 0.2%)

$THD$ of current in the 3rd phase versus motor torque under the adjusted levels of voltage unbalance is shown in Fig. 10. As regards lower levels of voltage unbalance, $THD_I$ is rather stable for a wide range of higher loads. It can be also seen a rising of $THD_I$ with unbalance rise, nevertheless, the level of distortion of current is still rather low, as can be seen better in Fig. 11.

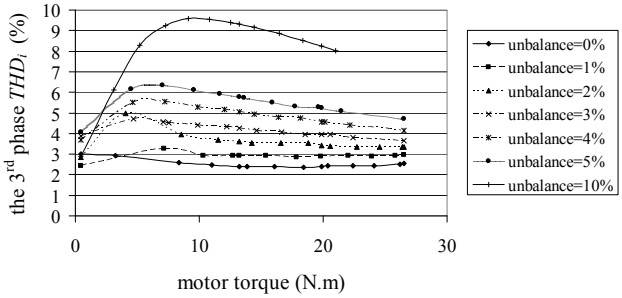


Fig.10. The 3rd phase current $THD$ versus motor torque under adjusted levels of voltage unbalance ($f$=50 Hz, $THD_V$ below 0.2%)

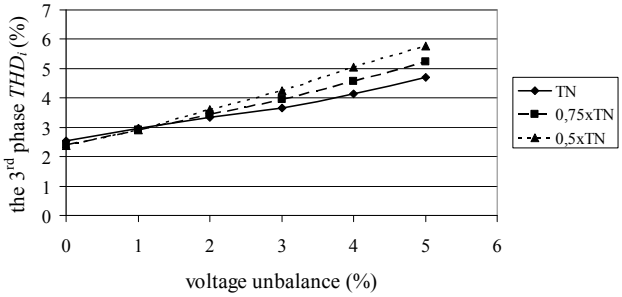


Fig.11. The 3rd phase current $THD$ versus voltage unbalance for chosen values of motor torque ($f$=50 Hz, $THD_V$ below 0.2%)

The reason of $THD_I$ increasing with voltage unbalance rise is obvious from both Fig. 12 for 50% load and Fig.13 for 100% load, where spectra of drawn current are displayed for the adjusted levels of voltage unbalance. As seen, the $THD_I$ rise is almost entirely caused by the rapid increasing of the 3rd harmonic current, while the other dominant harmonics of the 5th and 7th order are relatively stagnant.

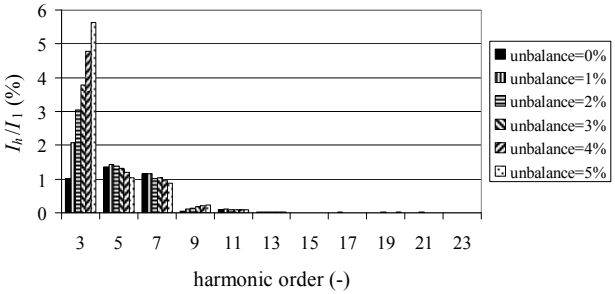


Fig.12. Spectrum of the 3rd phase current for adjusted levels of voltage unbalance (50% load, *f*=50 Hz, $THD_V$ below 0.2%)

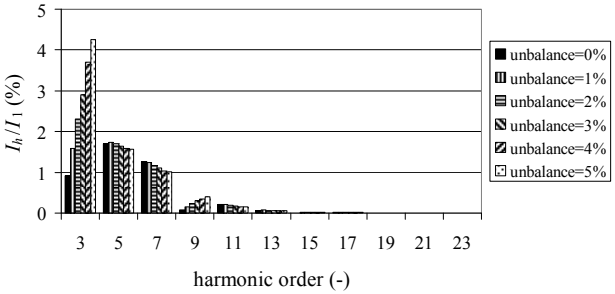


Fig.13. Spectrum of the 3rd phase current for adjusted levels of voltage unbalance (100% load, *f*=50 Hz, $THD_V$ below 0.2%)

However, the values of the 3rd harmonic remain very low in comparison with the fundamental one, not exceeding 6% of it for 50% load and 5% for 100% load respectively. So the current waveform is rather close to the sinusoidal one as can be seen in Fig. 14 or Fig. 15 for voltage unbalance of 2%.

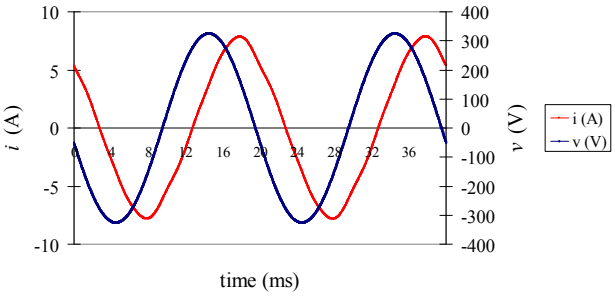


Fig.14. Waveforms of the 3rd phase current and voltage (2% unbalance, 50% load, *f*=50 Hz, $THD_I$ =3.6%, $THD_V$ below 0.2%)

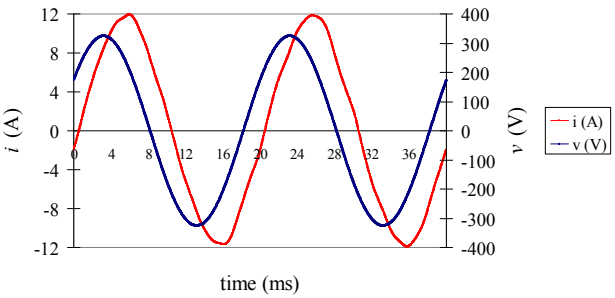


Fig.15. Waveforms of the 3rd phase current and voltage (2% unbalance, 100% load, *f*=50 Hz, $THD_I$ =3.35%, $THD_V$ below 0.2%)

**Some results from motor simulation model**

As mentioned above the induction motor parameters are asymmetric resulting in current unbalance even if the supply voltage is purely balanced. Machine parameters necessary as input data for simulation model such as coil leakage inductances, magnetising inductances and resistances are not identical in each motor phase, so they have a certain level of asymmetry. EMTP-ATP program enables to create a simulation model of cage rotor induction machine based on T-type equivalent circuit which is symmetrical with a possibility of approximation for saturation. If the model without saturation is used, the drawn current is sinusoidal in the case of sinusoidal supply voltage. This does not match the results obtained from experimental measurements due to the machine non-linearity. Saturation can be adopted into machine simulation model. However, its approximation is simple, piecewise-linear. The parameters used to define this segmented magnetization curve are residual flux-linkage, flux-linkage at the saturation knee point and saturated inductance. With respect to the behaviour of the magnetization curve of the tested motor its simple approximation only brings moderate increasing of drawn current distortion with comparison to the model without saturation.

The tested motor has the following parameters in the direct and quadrature axis:

Stator resistance: $R_d = R_q = 2{,}225\ \Omega$
Stator leakage inductance: $L_d = L_q = 0{,}01014$ H
Magnetising branch inductance: $L_{mud} = L_{muq} = 0{,}1727$ H
Rotor resistance: $R_1 = R_2 = 1{,}149\ \Omega$
Rotor leakage inductance: $L_1 = L_2 = 0{,}01014$ H

Waveforms of voltage and current in one phase of balanced three-phase system in simulation model are shown in Fig. 16, electromagnetic torque and angular velocity of rotor in Fig. 17.

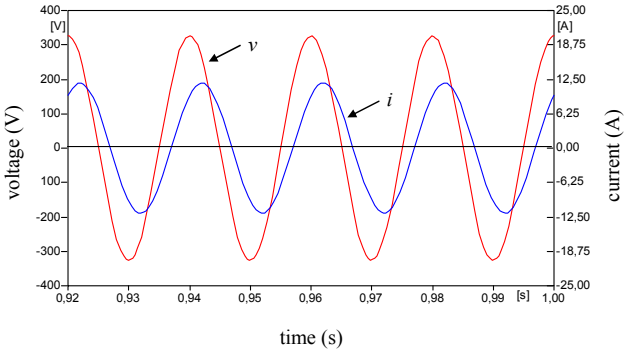


Fig.16. Waveforms of drawn current and voltage (balance, 100% load, *f*=50 Hz, $THD_V$ =0%)

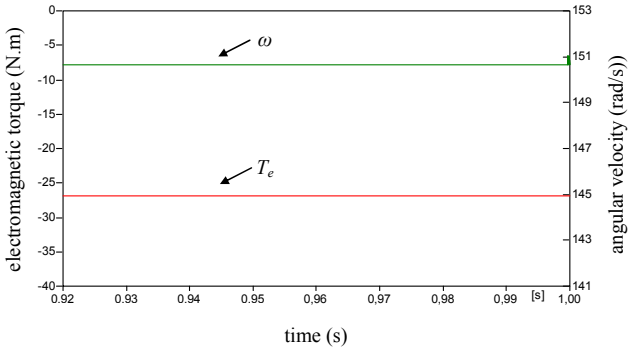


Fig.17. Electromagnetic torque and angular velocity (balance, 100% load, *f*=50 Hz, $THD_V$ =0%)

First, in table 2 the catalogue value of nominal speed is compared to the one obtained from experimental measurement and simulation under the nominal torque. Measured and simulated part of mechanical characteristics for balanced voltages and voltage unbalance equal to 10% are compared and shown in Fig. 18.

Table 2. Comparison of motor nominal speed

| | catalogue | measured | simulated |
|---|---|---|---|
| Nominal speed (rpm) | 1440 | 1439,5 | 1438,6 |

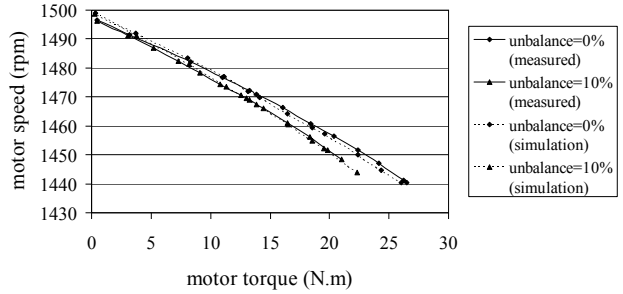


Fig.18. Comparison of measured and simulated motor mechanical characteristics

In table 3 the values of nominal current and power factor are compared.

Table 3. Comparison of motor nominal current and power factor

| | catalogue | measured | simulated |
|---|---|---|---|
| Nominal current (A) | 8,2 | 8,56 | 8,35 |
| Nominal *PF* (-) | 0,81 | 0,804 | 0,813 |

Measured and simulated current unbalance versus adjusted levels of voltage unbalance is presented in Fig. 19. As seen, in the case of the balanced system simulations give results of current unbalance virtually 0% in contrast to the measured values.

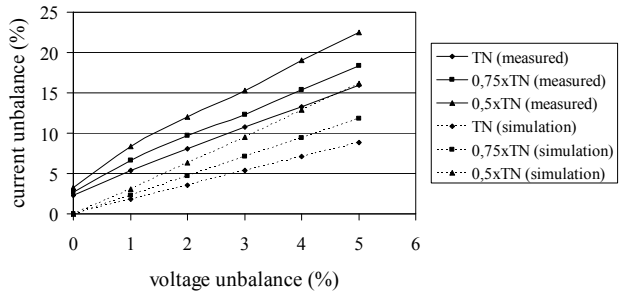


Fig.19. Current unbalance versus voltage unbalance for chosen values of motor torque (measured and simulated)

A simulated current distribution in phases is in Fig. 20 for voltage unbalance equal to 2% and is close to the measured one presented in Fig. 6. However, the current differences for given torque are less than at measured results. The drawn current is also marked in it in the case of balanced system.

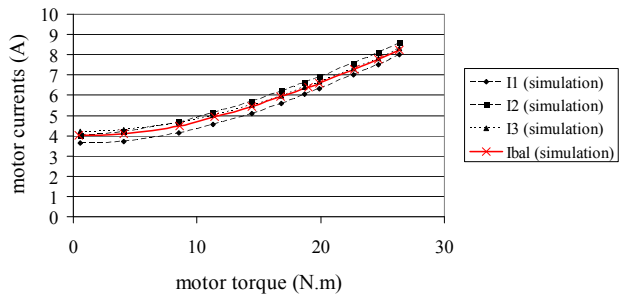


Fig.20. Simulated motor phase currents versus motor torque under voltage unbalance of 2%

A comparison of the measured and simulated current in the 2nd phase, where both currents have the highest value is presented in Fig. 21 under chosen levels of unbalance.

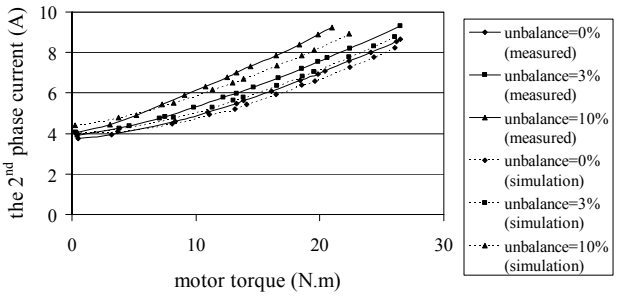


Fig.21. The 2nd phase motor current versus motor torque under chosen levels of voltage unbalance (measured and simulated)

## Conclusion

In this paper results of experimental measurements of 4kW three-phase squirrel cage motor are presented and some of them compared to results of computer simulations using EMTP-ATP program. A dependence of some motor parameters on voltage unbalance such as efficiency, speed and currents including their unbalance and distortion has been tested. As seen in figures, motor efficiency and speed are not almost reduced by lower levels (c. up to 2%) of voltage unbalance. As expected, it has the higher influence on current values and their distribution in phases resulting in higher current unbalance, and also on current distortion.

The model of induction motor used in EMTP-ATP program matches the tendency of some parameters depending on loading or voltage unbalance rather well. Nevertheless, due to the model design and its possibilities there are higher differences in comparison with measured values, which is more evident at current unbalance and mainly at current distortion.

*This work was supported by the SGS FEI, VŠB-TU Ostrava under Grant SP 2012/41*

## REFERENCES

[1] IEC 1000 2-1, Electromagnetic compatibility (EMC) - Part 2-1: Environment – Description of the environment – Electromagnetic environment for low frequency conducted disturbances and signaling in public power supply systems, (1993) 1-18

[2] EN50160, Voltage characteristics of electricity supplied by public electricity networks, (2011), 1-32

[3] Auinger H., Bunzel E., Friedrich K., Determining the efficiency of electric motors, Energy Efficiency in Motor Driven Systems – 2003, (2003), 7p.

[4] Deprez W., Göl O., Belmans R., Vagaries of efficiency measurement methods for induction motors, *In Proc. of Energy Efficiency in Motor Driven Systems Conf. (EEMODS)*, (2005), vol. 1, 158 - 168

[5] Faiz J., Influence of unbalanced voltage on the steady-state performance of a three-phase squirrel-cage induction motor, *In IEEE Transactions on Energy Conversion,* (2004) vol. 19, No. 4, 657-662

[6] Mzungu H. M., Sebitosi A. B., Khan M. A., Comparison of standards for determining losses and efficiency of three-phase induction motors, *In Proc. of IEEE PES Power Africa 2007 Conference*, (2007), 6p.

[7] Sandhu S. K., Chaudhary V., Simulations of three-phase induction motor operating with voltage unbalance, *In Proc. of Conf. on Electric Power Systems, High Voltages, Electric Machines,* (2008), 273-279

[8] EN 60034-26, Effects of unbalanced voltages on the performance of three-phase cage induction motors,(2007), 1-10

***Authors:*** *doc. Ing. Stanislav Kocman, Ph.D.; Ing. Petr Orság, Ph.D.; Ing. Jan Šmída, VŠB-Technical University of Ostrava, FEECS, Dept. of Electrical Engineering,17. listopadu 15, 708 33 Ostrava-Poruba, Czech Republic, E-mail: stanislav.kocman@vsb.cz; petr.orsag@vsb.cz; jan.smida@vsb.cz.*